

Supporting Information for

Generation of local redox potential from confined nano-bimetals in porous metal silicate materials for high-performance catalysis

Yang-Yang Liu, Xiao-Ke Shi and Chuan-De Wu*

State Key Laboratory of Silicon Materials, Department of Chemistry, Zhejiang University, Hangzhou, 310027, P. R. China

Email: cdwu@zju.edu.cn

Experimental Section

Materials

Cobalt chloride hexahydrate (99%), nickel perchlorate hexahydrate (99%), sodium benzoate (99%), triethylamine (99.5%), hydroxymethylpyridine (98%, hmp-H), boric acid (99%), tetraethyl orthosilicate (99%, TEOS) and naphthalene (98%) were supplied by Saan Chemical Technology Co., Ltd (Shanghai, China). Isopropanol (99.7%) and heptane (97%) were supplied by Sinopharm Chemical Reagent Co. Ltd (China). High purity hydrogen (99.999%), high purity nitrogen (99.999%), high purity argon (99.999%), 10% H₂/Ar and 7% NH₃/Ar were supplied by Hangzhou Jingong Materials Co. Ltd (China). All other reagents used in this work are of analytical grade, which were directly used without further purification.

Preparation of PMS-16

PMS-16 was prepared by employing sol-gel method. Sodium benzoate (2.5 mmol) and Ni(ClO₄)₂·6H₂O (1 mmol) were dissolved in 30 mL of methanol under stirring. CoCl₂·6H₂O (1 mmol), Et₃N (2 mmol) and hmp-H (2 mmol) were successively added into the mixture under stirring. The mixture was further reacted at room temperature for 4 h, resulting a coordination complex, abbreviated as {NiCo}. Subsequently, TEOS (3.5 mL, Si : metal = 8 : 1) and boric acid (2 mmol) were dropwise added into the {NiCo} solution, which was stirred until formation of gel at room temperature.

The resulting gel was transferred into a Teflon-lined autoclave, which was reacted at 120 °C for 48 h. The resulting solid was collected, dried and annealed at different temperatures (300, 400, 500, 600 and 700 °C) under N₂ atmosphere for 2 h.

Scaled preparation of PMS-16. Sodium benzoate (0.25 mol) and Ni(ClO₄)₂·6H₂O (0.1 mol) were dissolved in 2.5 L of methanol under stirring. CoCl₂·6H₂O (0.1 mol), Et₃N (0.2 mol) and hmp-H (0.2 mol) were successively added into the mixture under stirring. The mixture was further reacted at room temperature for 4 h, resulting coordination complex {NiCo}. Subsequently, TEOS (350 mL) and boric acid (0.2 mol) were dropwise added into the {NiCo} solution, which was stirred until formation of gel at room temperature. The resulting gel was transferred into a Teflon-lined autoclave, which was reacted at 120 °C for 48 h. The resulting solid was collected, dried and annealed at 600 °C under N₂ atmosphere for 2 h.

Catalyst characterization

Transmission electron microscopy (TEM, HT7700 and JEM 2100F) and scanning electron microscope (SEM, Hitachi S-4800) were used to characterize the morphology of PMS-16. Powder X-ray diffraction (PXRD) data were recorded on a RIGAKU D/MAX 2550/PC with Cu K α radiation ($\lambda = 1.5406 \text{ \AA}$). FT-IR spectra were collected from KBr pellets on an FTS-40 spectrophotometer. Thermogravimetric analysis (TGA) was carried out under N₂ atmosphere on a NETZSCH STA 409 PC/PG instrument at a heating rate of 10 °C min⁻¹. Inductively coupled plasma mass spectrometry (ICP-MS) was performed on an X-Series II instrument. A Micromeritics ASAP 2020 surface area analyzer was used to measure N₂ gas adsorption/desorption isotherms. Pulse CO chemisorption measurements were carried out on a Micromeritics AutoChem 2920 instrument. A PMS-16 sample was pre-reduced in H₂ atmosphere at 500 °C with a heating rate of 10 °C min⁻¹, which was subsequently cooled down to 50 °C for CO chemisorption analysis by introducing successive pulse doses of 5% CO-He gas. X-ray photoelectron spectra (XPS) were recorded on a VG ESCALAB MARK II machine. Temperature-programmed reduction of H₂ (H₂-TPR) and temperature-programmed desorption of NH₃ (NH₃-TPD) were conducted on VDsorb-

91i instrument. Temperature-programmed oxidation (TPO) experiments were conducted on AutoChem1 II 2920. The conversion and chemoselectivity for the hydrogenation reaction were based on the GC-MS analysis results.

Electrochemical measurements

5.0 mg catalyst was dispersed in 500.0 μL ethanol and 50.0 μL 0.5 wt% nafion solution, and followed by intense sonication for 0.5 h, resulting a homogeneous catalyst ink. The ink was deposited onto carbon paper and dried, which were used as the working electrodes in a dual chamber cell system.

Cyclic voltammetry experiments were performed using a three-electrode cell with a CHI660E electrochemical workstation at ambient temperature. 3.0 mg catalyst was dispersed in 300.0 μL ethanol and 30.0 μL 0.5 wt% nafion solution, followed by intense sonication for 0.5 h, resulting a homogeneous catalyst ink. 30.0 μL ink was deposited onto carbon paper and dried to form a uniform thin film, which was used as the working electrode. Cyclic voltammograms were recorded with a scan rate of 10 mV s^{-1} in 1 M KOH aqueous solution by using saturated Ag/AgCl electrode as the reference electrode.

Catalytic hydrogenation

Catalytic hydrogenation of naphthalene was performed in a 50 mL autoclave lined with polytetrafluoroethylene (PTFE). PMS-16 was activated before catalyzing the hydrogenation reaction by reducing in H_2 atmosphere (1 atm) at 500 $^\circ\text{C}$ for 1 h. In a typical experimental procedure, 0.05 mmol of naphthalene in 0.5 mL heptane, PMS-16 (10.0 mol% based on Co and Ni) and 4 mL of isopropanol were added into the autoclave. Hydrogen gas (1.5 MPa) was injected into the reactor five times to remove the dissolved air. The autoclave was heated at 120 $^\circ\text{C}$ in an oil bath for 8 h. The solid catalyst was separated by centrifugation, and the products were analyzed by GC-MS. The major products were calibrated by using standard curves. All catalytic reactions were performed twice and the reported results are the average values.

The reaction conditions for studying the kinetic behaviors of different catalysts in the hydrogenation reaction at different temperatures: naphthalene (1 mmol), catalyst (0.5 mol% based on Co and Ni), heptane (1 mL) and isopropanol (8 mL), 8 h, 1.5 MPa H₂.

The reaction conditions for selective hydrogenation of naphthalene catalyzed by different control catalysts, which were prepared by directly pyrolyzing the corresponding coordination complexes: naphthalene (0.1 mmol), catalyst (25.0 mol% based on Ni or Co), heptane (0.5 mL) and isopropanol (4 mL), 8 h, 120 °C, 1.5 MPa H₂.

Figures

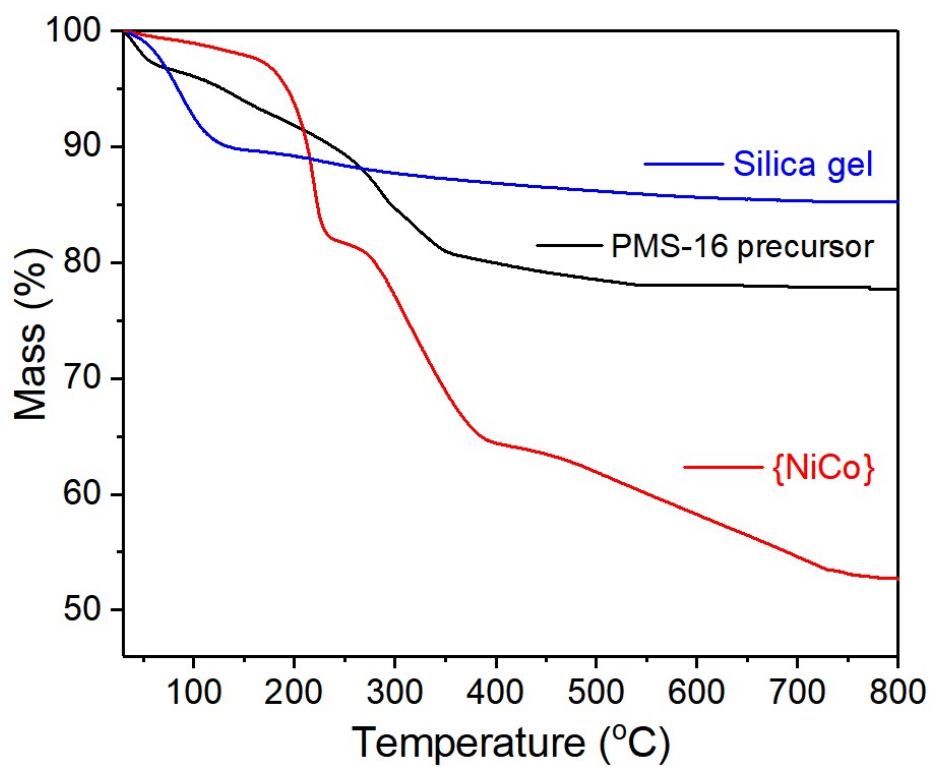


Fig. S1 TGA curves for silica gel, coordination complex {NiCo} and the PMS-16 precursor.

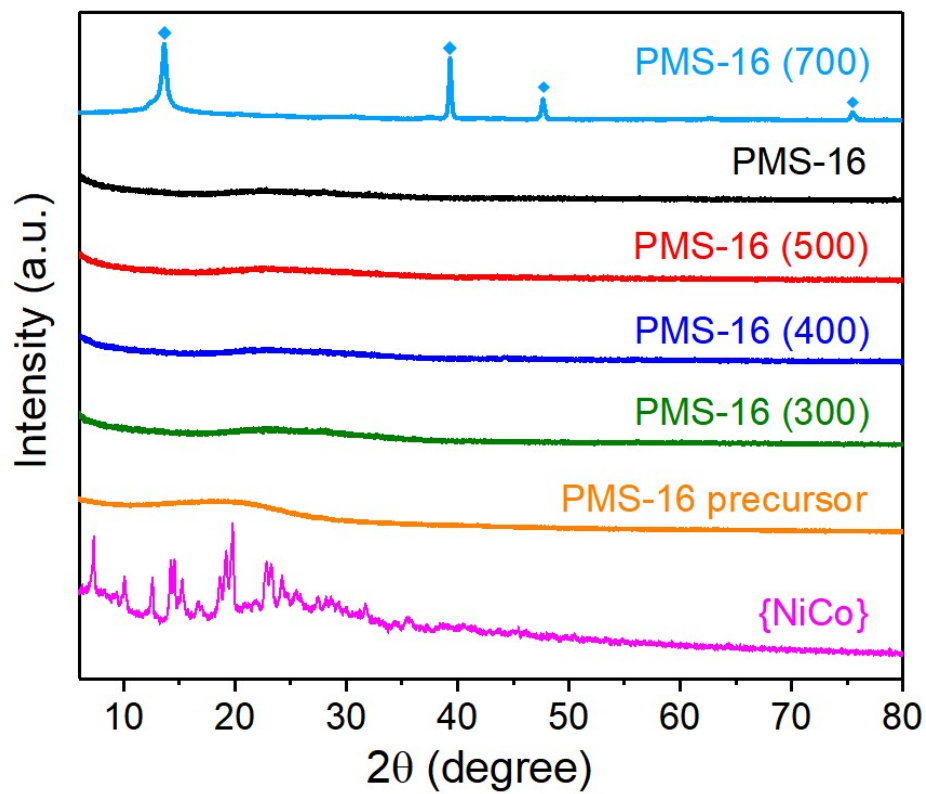


Fig. S2 PXRD profiles of the PMS-16 precursor and the annealed products at different temperatures (the numbers in the parentheses represent the annealing temperature).

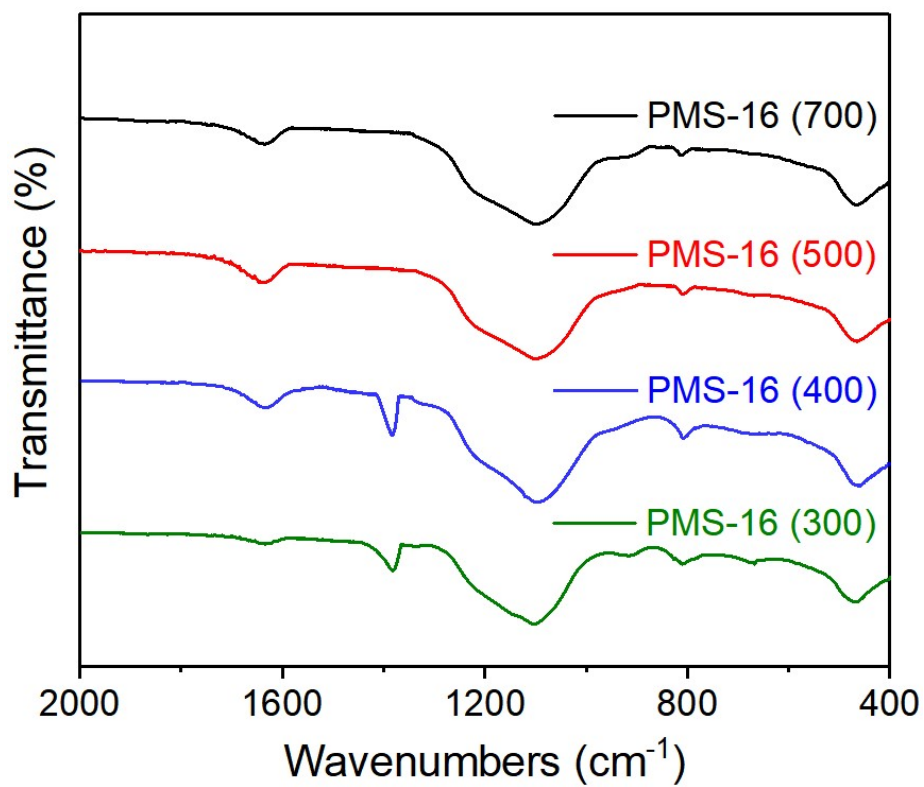


Fig. S3 FT-IR spectra of the annealed products of the PMS-16 precursor at different temperatures.

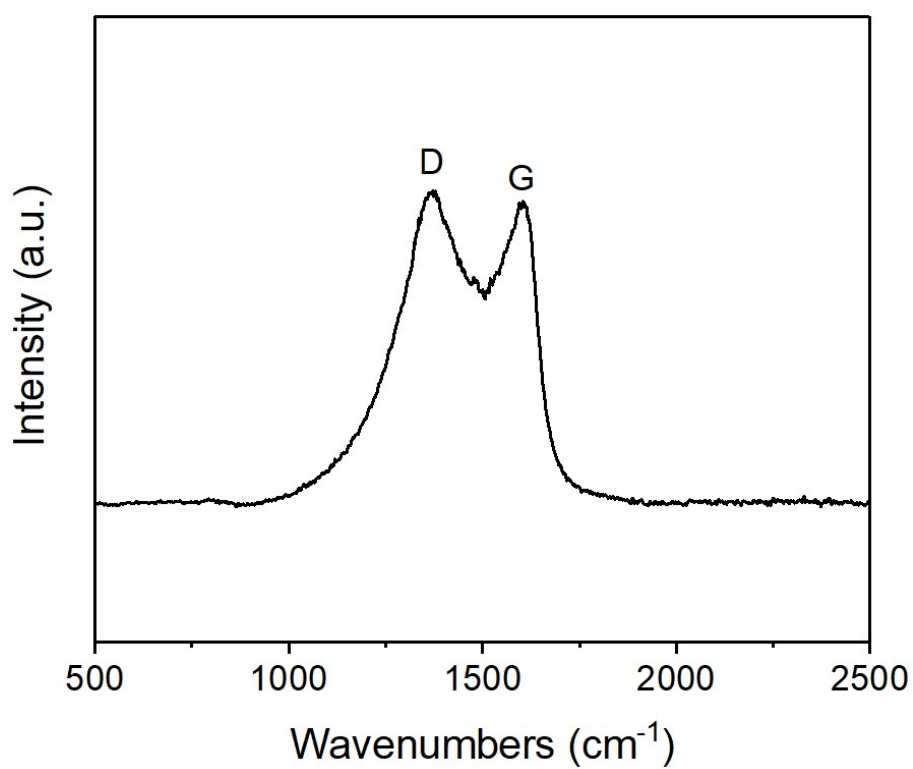


Fig. S4 Raman spectrum of PMS-16 (700).

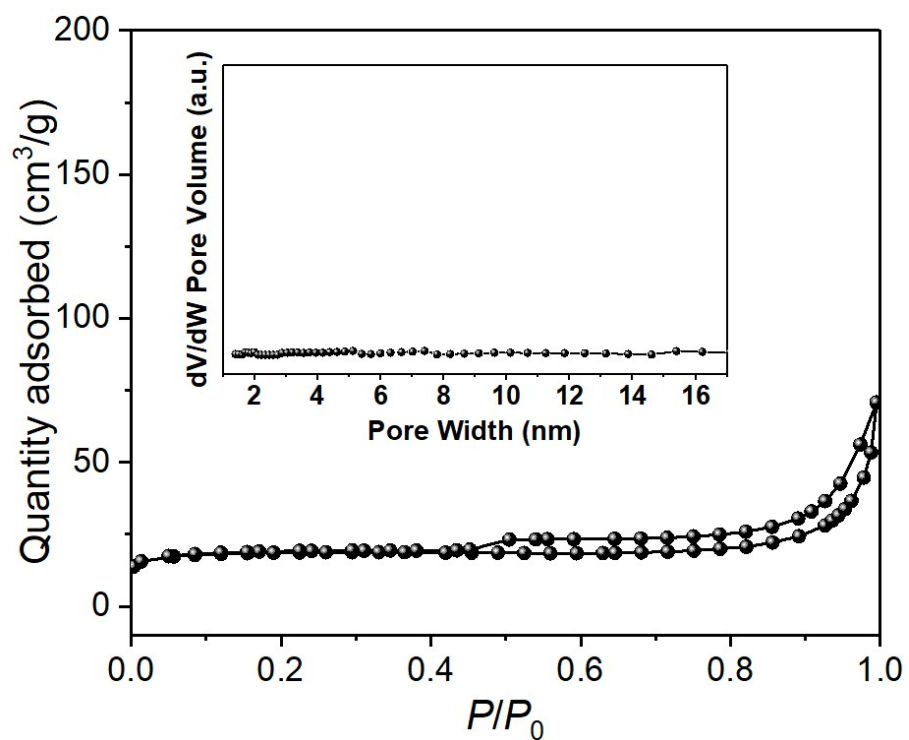


Fig. S5 Nitrogen adsorption/desorption isotherms for the PMS-16 precursor (the insert shows the pore size distribution for the PMS-16 precursor).

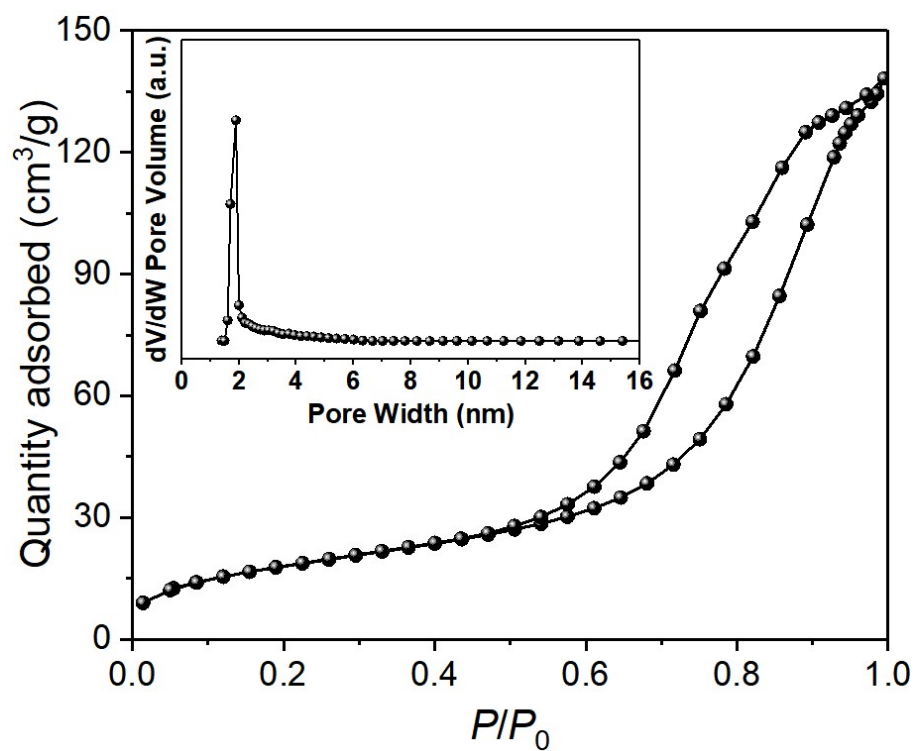


Fig. S6 Nitrogen adsorption/desorption isotherms for PMS-16 (300) (the insert shows the pore size distribution for PMS-16 (300)).

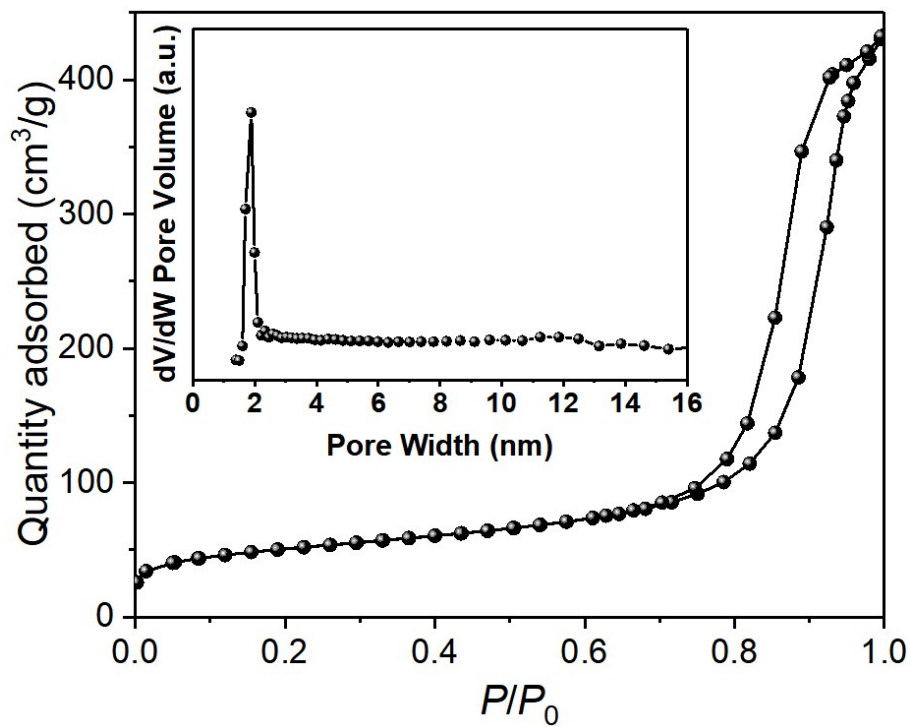


Fig. S7 Nitrogen adsorption/desorption isotherms for PMS-16 (400) (the insert shows the pore size distribution for PMS-16 (400)).

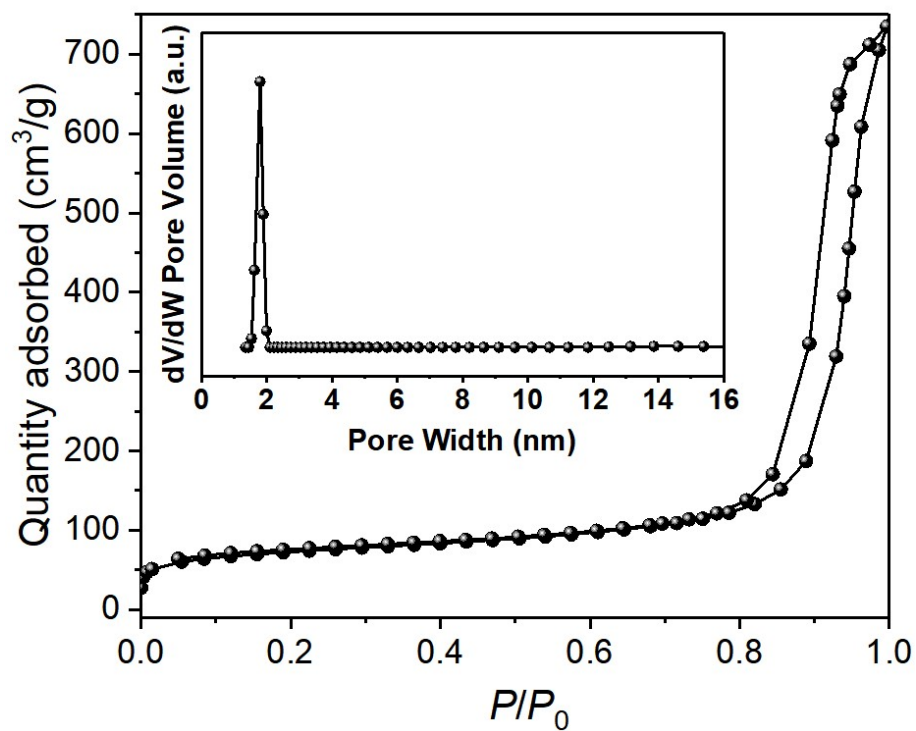


Fig. S8 Nitrogen adsorption/desorption isotherms for PMS-16 (500) (the insert shows the pore size distribution for PMS-16 (500)).

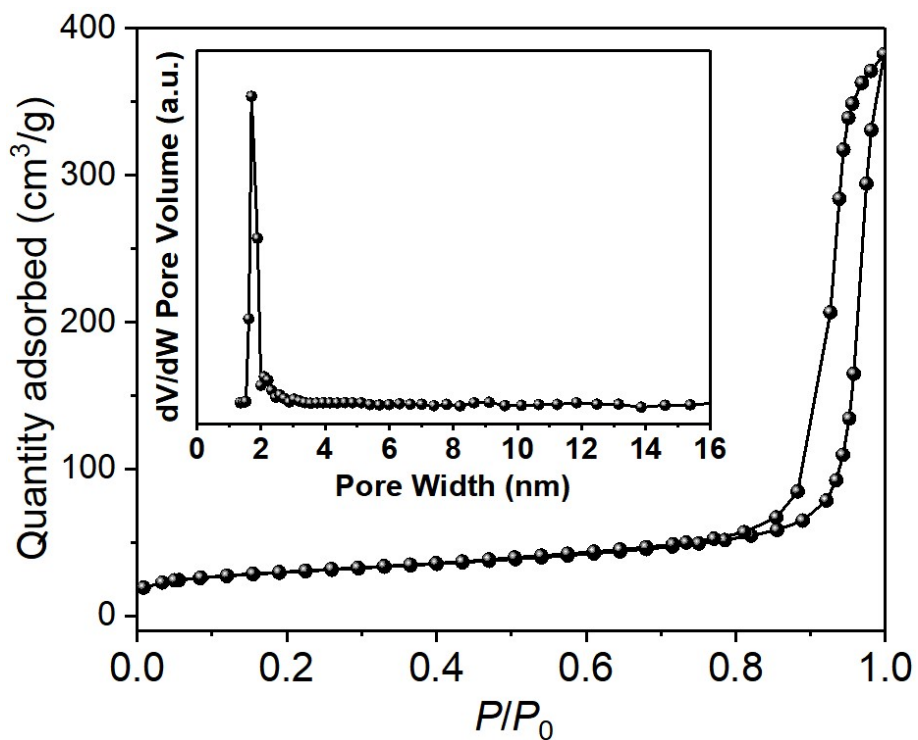


Fig. S9 Nitrogen adsorption/desorption isotherms for PMS-16 (700) (the insert shows the pore size distribution for PMS-16 (700)).

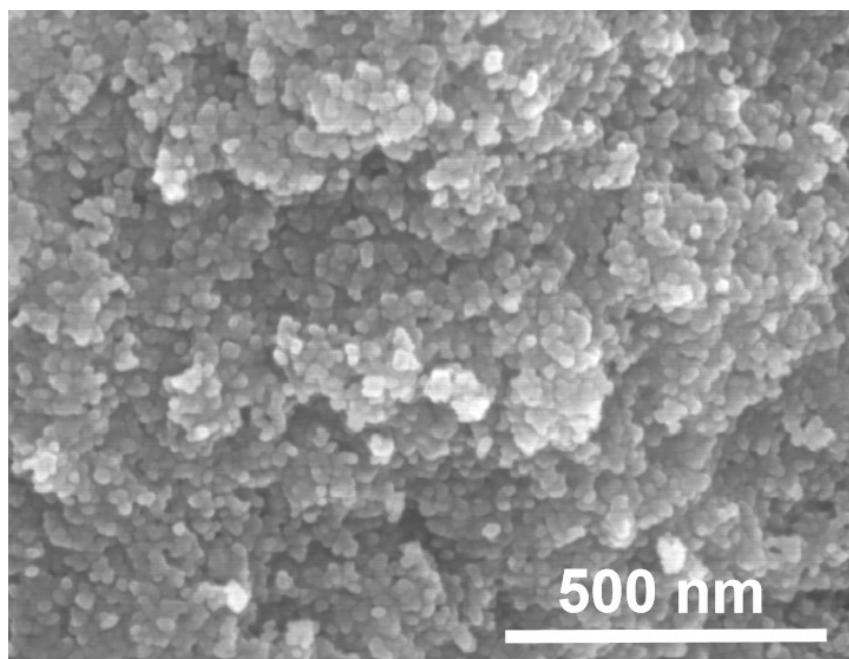


Fig. S10 SEM image of the PMS-16 precursor.

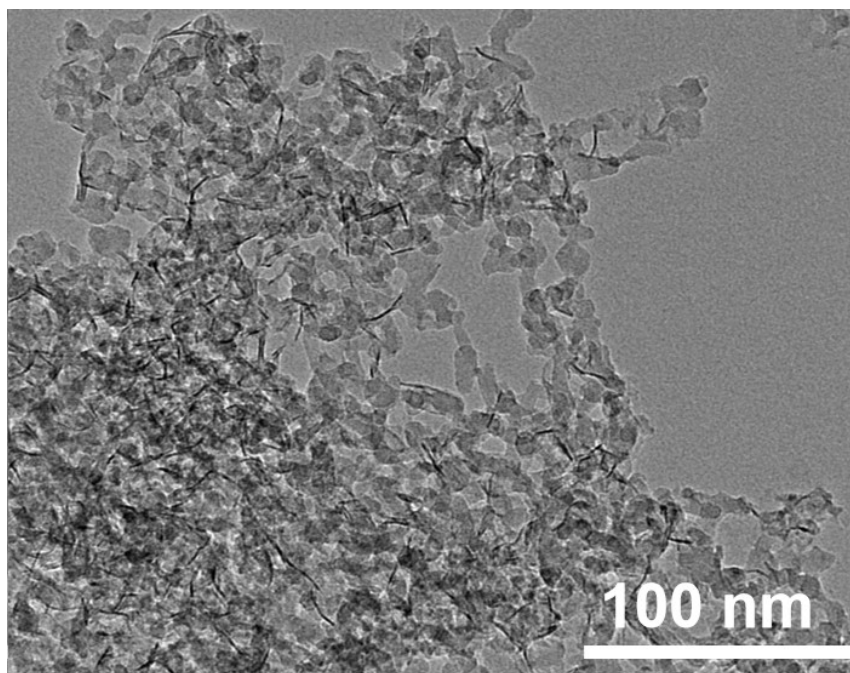


Fig. S11 HR-TEM image of the PMS-16 precursor.

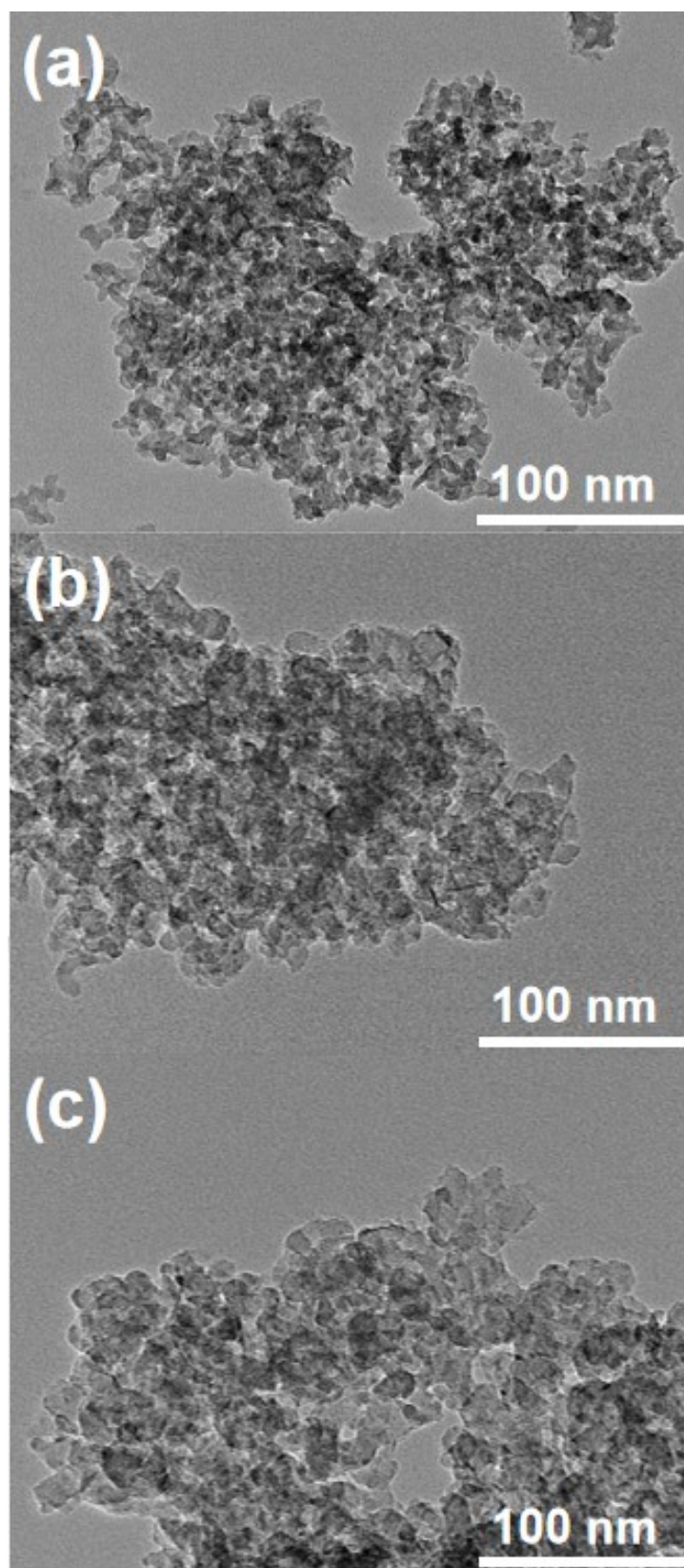


Fig. S12 HR-TEM images of (a) PMS-16 (300), (b) PMS-16 (400) and (c) PMS-16 (500).

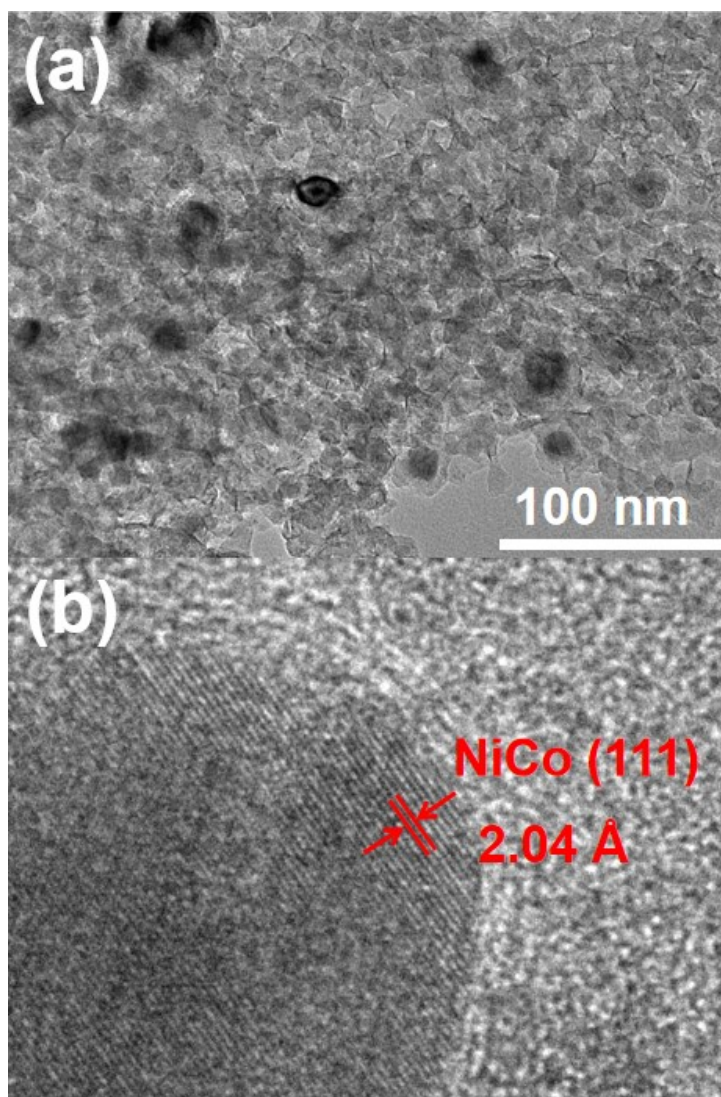


Fig. S13 HR-TEM image of PMS-16 (700).

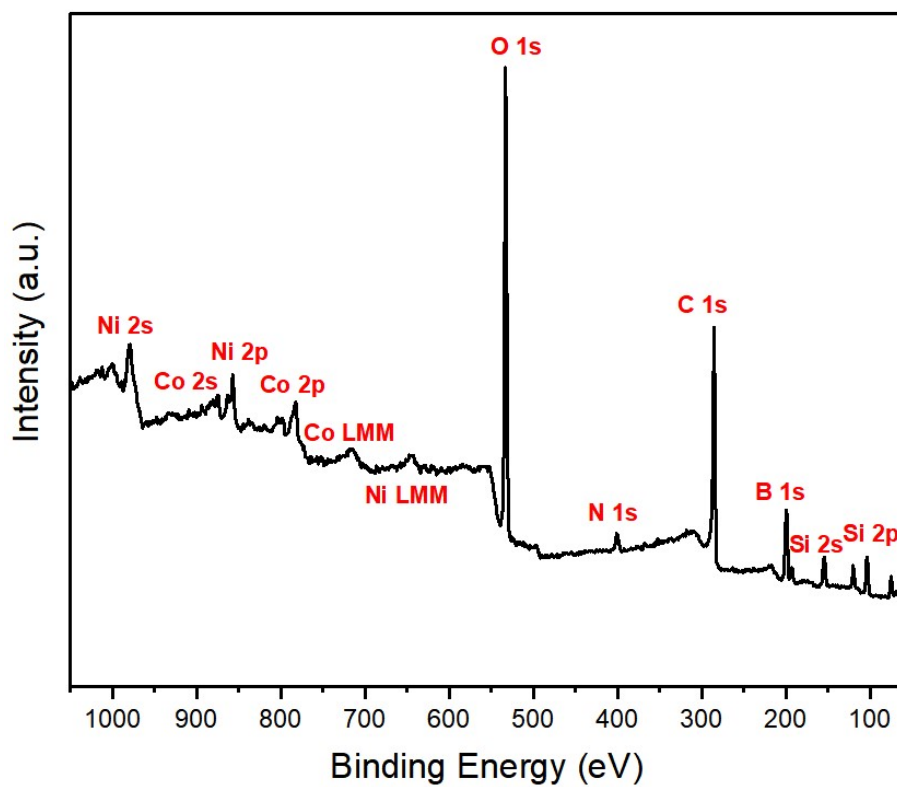


Fig. S14 XPS spectrum of PMS-16.

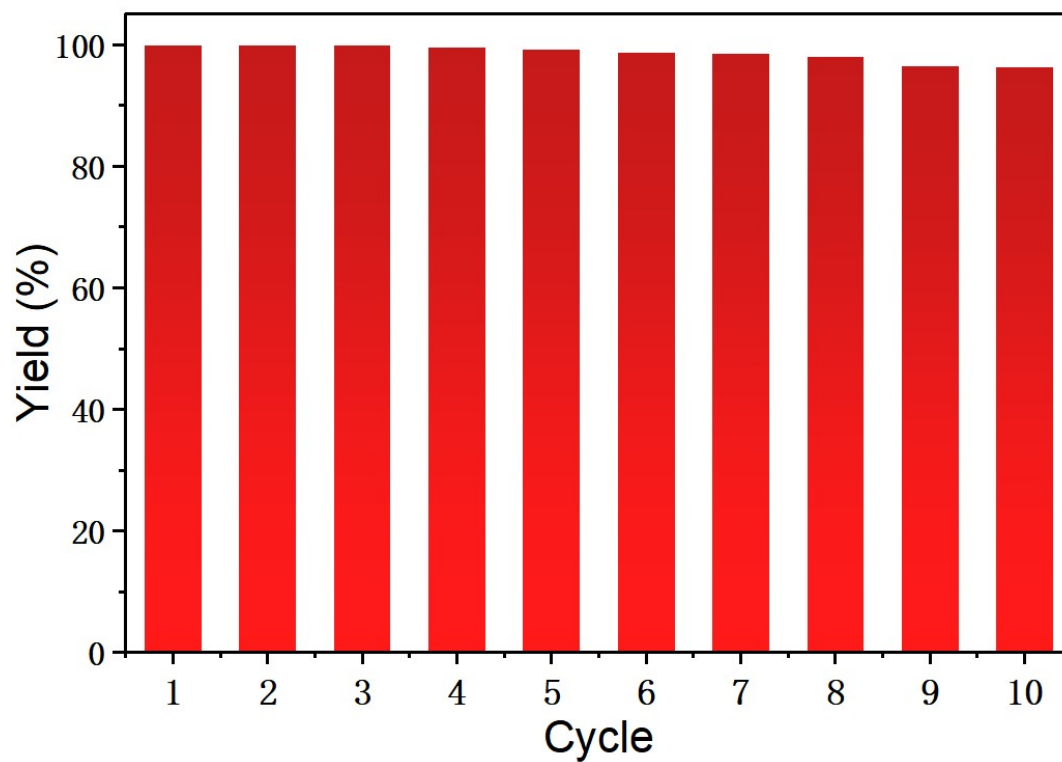


Fig. S15 Catalytic reusability test for PMS-16. Reaction conditions: naphthalene (0.05 mmol), catalyst (10.0 mol% based on Ni and Co), heptane (0.5 mL) and isopropanol (4 mL), 8 h, 120 °C, 1.5 MPa H₂.

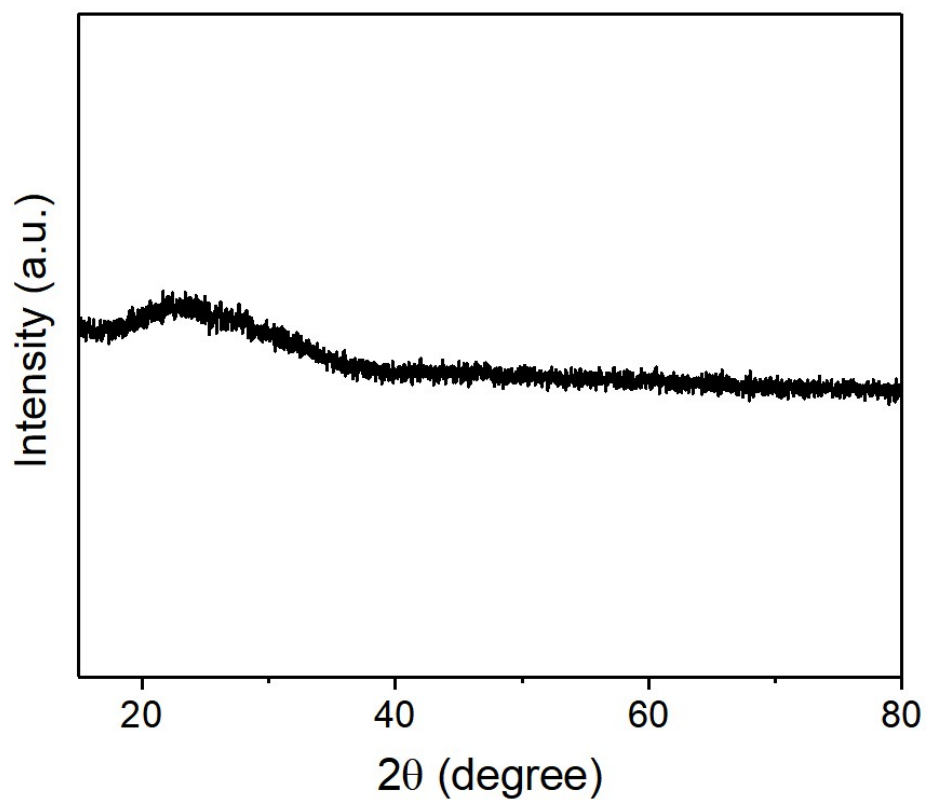


Fig. S16 PXRD profile of PMS-16 after catalysis.

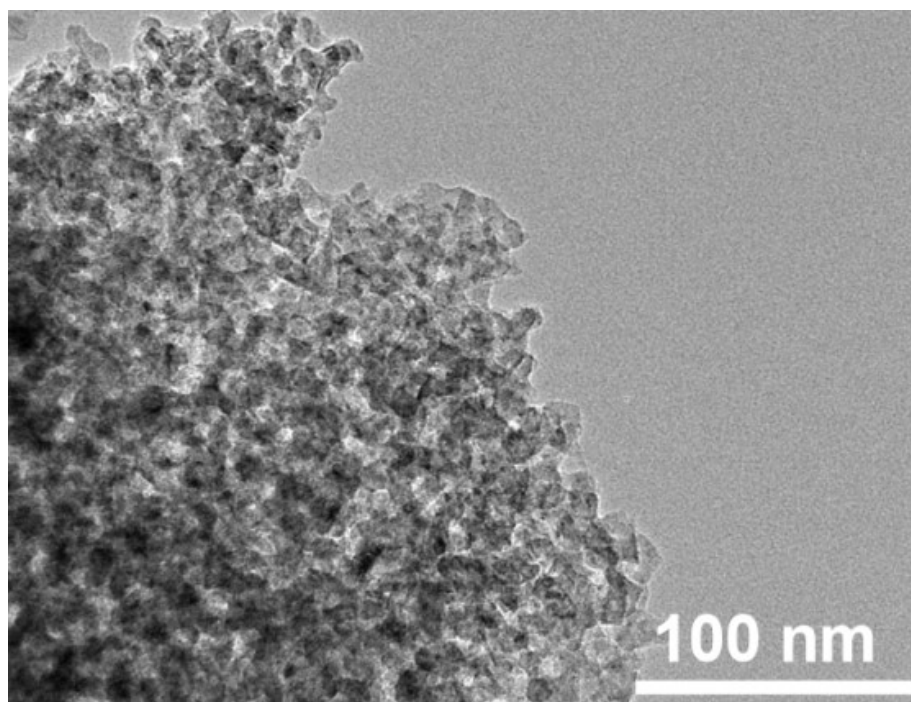


Fig. S17 HR-TEM image of PMS-16 after catalysis.

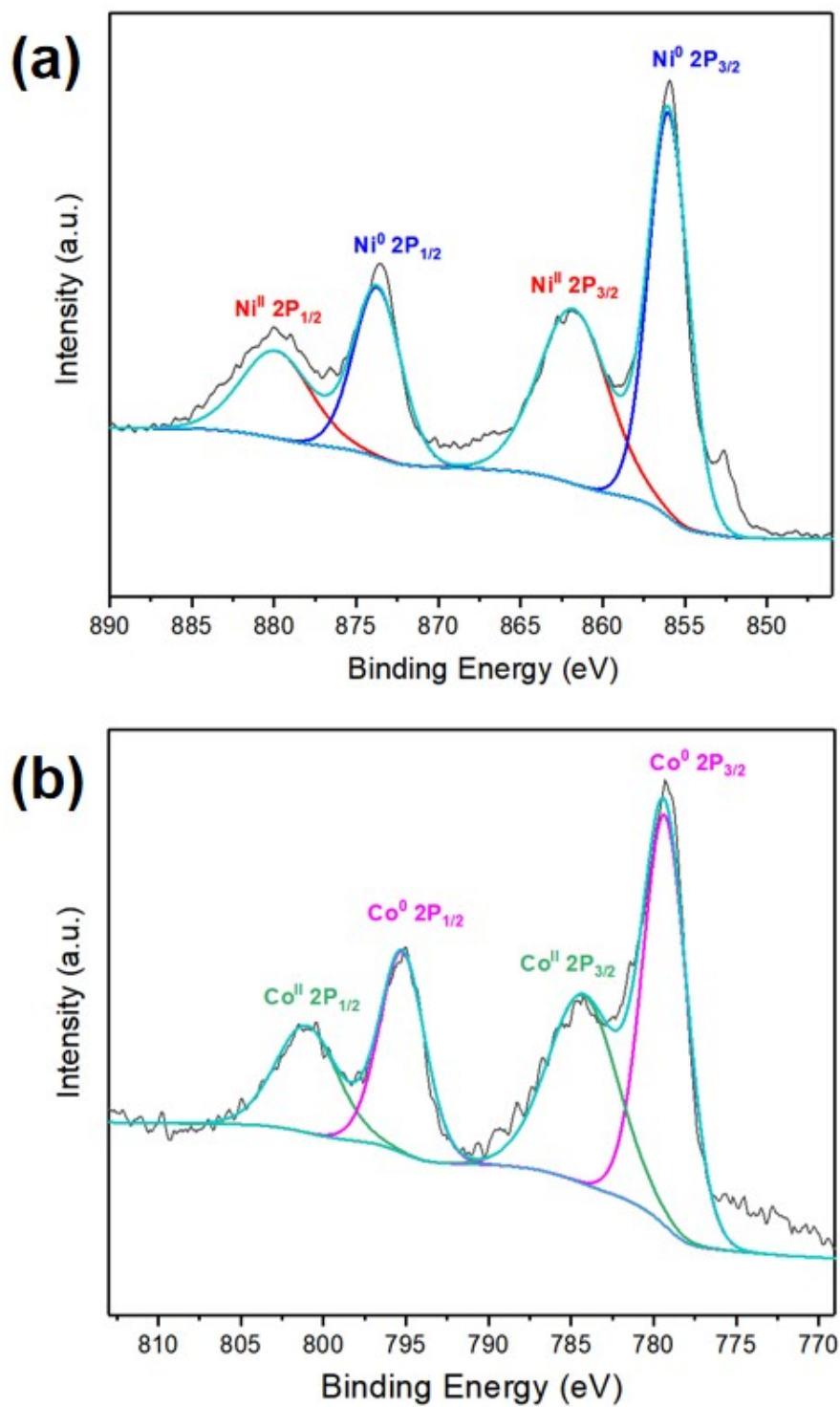


Fig. S18 High resolution (a) Ni 2p and (b) Co 2p XPS spectra of PMS-16 after catalysis.

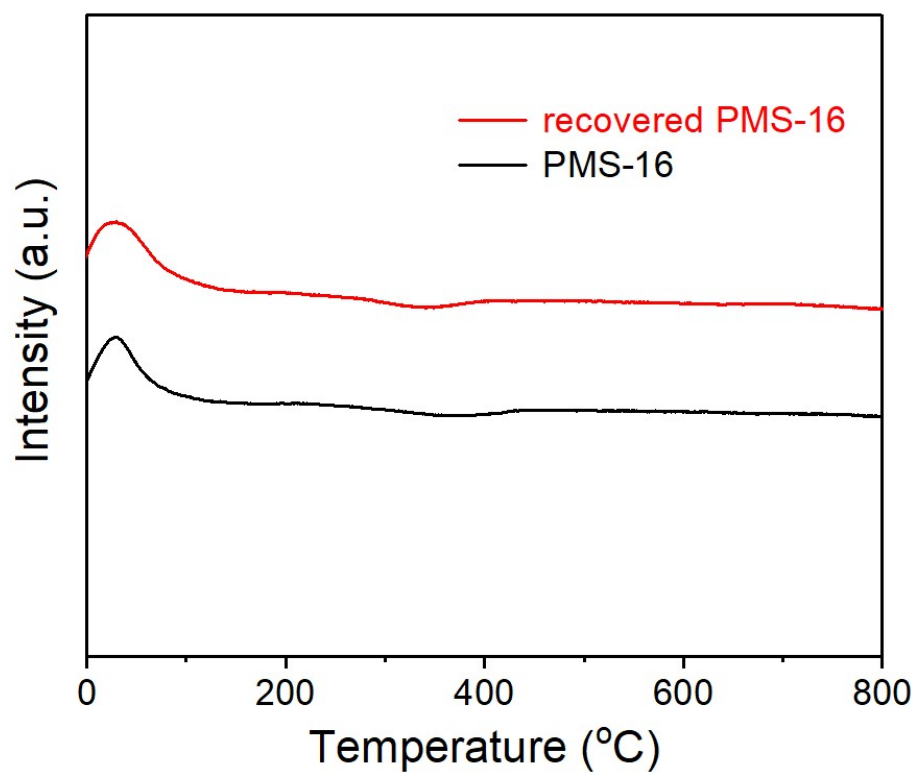


Fig. S19 Temperature-programmed oxidation (TPO) profiles of PMS-16 and recovered PMS-16 after catalysis.

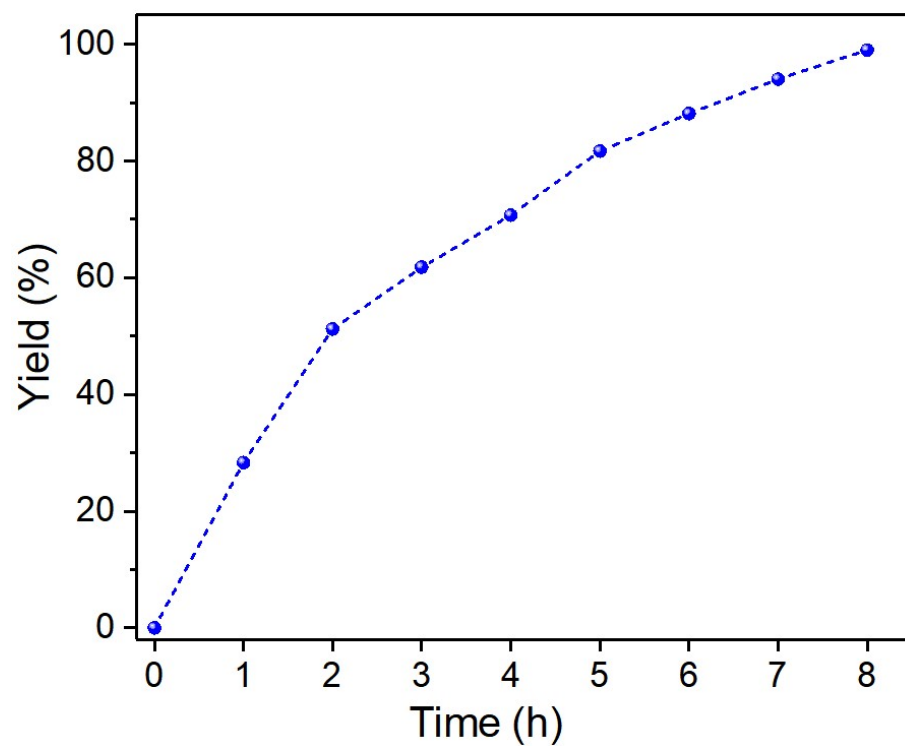
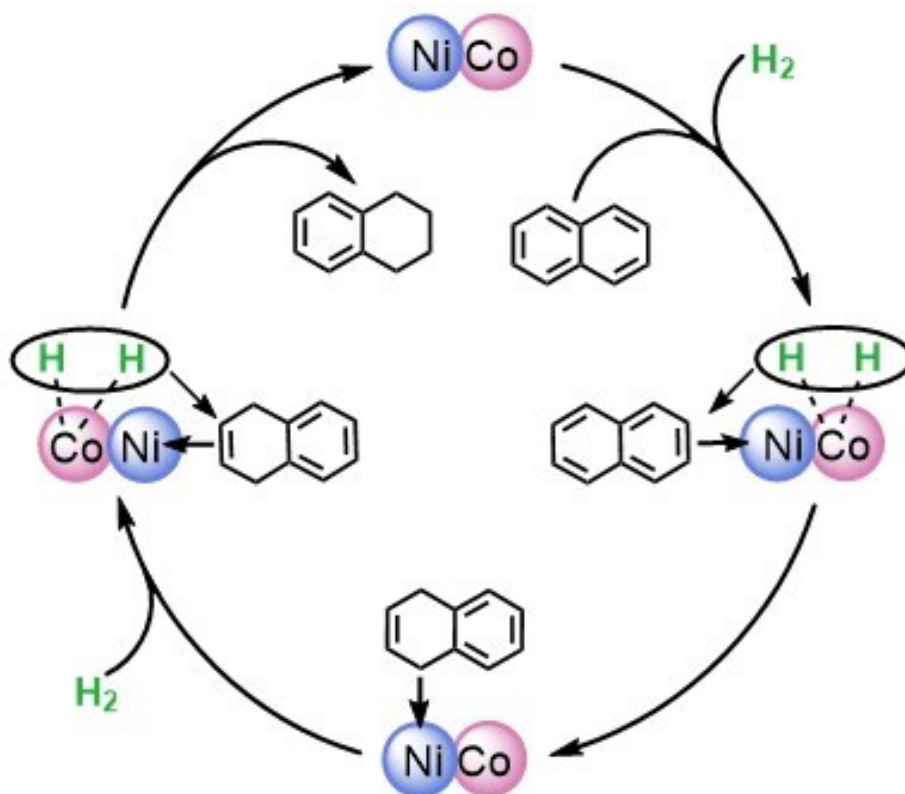


Fig. S20 Catalytic performance of PMS-16 for hydrogenation of naphthalene at 120 °C.



Scheme S1 A plausible catalytic pathway for hydrogenation of naphthalene catalyzed by PMS-16.

Tables

Table S1. Textural properties of different materials

Material	Co (wt%) ^a	Ni (wt%) ^a	S _{BET} (m ² g ⁻¹) ^b	Pore Size (nm) ^b
PMS-16 precursor	1.0	1.0	56.8	-
PMS-16 (300)	1.9	2.0	141.0	1.89
PMS-16 (400)	2.0	1.9	230.3	1.89
PMS-16 (500)	2.0	2.0	326.1	1.89
PMS-16	2.0	2.0	427.3	1.89
PMS-16 (700)	2.0	2.1	132.1	1.89

^aDetermined by ICP-MS. ^bDetermined by multipoint BET method.

Table S2. CO adsorption properties over different PMS materials

Material	CO uptake ($\mu\text{mol/g}$) ^a	Dispersion (%) ^b	Metal surface area (m^2/g) ^c	Particle size (nm) ^d
PMS-16	64.1	18.9	125.6	5.4
recovered PMS-16	62.0	18.3	121.5	5.5

^aEstimated from the area under the CO pulse signals.

^bCalculated from the CO uptake using equation: $(V \times \text{S.F.} \times \text{M.W.})/(\text{c}/100) \times 100$; where V is the amount of CO uptake (mol/g), S.F. is the stoichiometric factor, M.W. is the average atomic weight of supported metal and c is the metal loading (wt%).

^cCalculated from the equation: $(V \times N_A \times \text{S.F.} \times \sigma_m \times 10^{-18})/\text{c} \times 100$; where N_A is the Avagadro number and σ_m is the average metal cross section area.

^dMean particle size calculated from the following equation: $60/(A_m \times \rho)$, where A_m is the metal surface area per gram catalyst and ρ is the average metal density.

Table S3. Quantities of acid sites in different PMS materials

Material	Weak acid sites ($\mu\text{mol/g}$)	Strong acid sites ($\mu\text{mol/g}$)	Total acid sites ($\mu\text{mol/g}$)
PMS-16 _{B-free}	4.67	5.29	9.96
PMS-16	18.97	3.51	22.48

Table S4. The catalytic performances of PMS-16 for selective hydrogenation of naphthalene in different solvents^a

Entry	Solvent	Time (h)	Conv. (%) ^b	Sel. (%) ^b
1	Methanol	6	39.0	>99
2	Ethanol	6	41.6	>99
3	Isopropanol	6	88.1	>99
4	Heptane	6	34.2	>99
5	Tetrahydrofuran	6	57.5	>99

^aReaction conditions: naphthalene (0.05 mmol), solvent (4 mL), PMS-16 (10.0 mol% based on Ni and Co), 120 °C, 1.5 MPa H₂. ^bDetermined by GC-MS.

Table S5. Selective hydrogenation of naphthalene catalyzed by different PMS materials^a

Entry	Catalyst	Conv. (%) ^b	Sel. (%) ^b
1	PMS-16 (300)	52.1	>99
2	PMS-16 (400)	94.6	>99
3	PMS-16 (500)	87.1	>99
4	PMS-16 (700)	35.5	>99
5	PMS-16a (Ni:Co = 2:1)	95.4	>99
6	PMS-16b (Ni:Co = 1:2)	81.4	>99
7	PMS-16c (Si:metal = 2:1)	73.7	>99
8	PMS-16d (Si:metal = 4:1)	89.2	>99
9	PMS-16 (Si:metal = 8:1)	>99	>99
10	PMS-16e (Si:metal = 16:1)	92.4	>99
11	Scale-prepared PMS-16	>99	>99

^aReaction conditions: naphthalene (0.05 mmol), catalyst (10.0 mol% based on Ni and Co), heptane (0.5 mL) and isopropanol (4 mL), 8 h, 120 °C, 1.5 MPa H₂. ^bDetermined by GC-MS.

Table S6. Comparison of the catalytic performances of different catalysts in the literature for selective hydrogenation of naphthalene to produce tetralin in autoclaves

Catalyst	T (°C)	P (MPa)	Time (h)	Conv. (%)	Sel. (%)	Ref.
Pd/USY	200	6.89	2	95	95	S1
Pd/Al-MCM-41	250	6.2	0.3	100	94.5	S2
Ni/ZSM-5	180	5	10	>95	>95	S3
Ru/PVPy	150	5	1	100	78	S4
Ru/MgO	150	5	-	95	80	S5
Pt/HAP	250	6	4	96	97	S6
PMS-16	120	1.5	8	>99	>99	This work

Table S7. Comparison of the catalytic performances of different catalysts in the literature for selective hydrogenation of naphthalene to produce tetralin in fixed-bed reactors

Catalyst	T (°C)	P (MPa)	Conv. (%)	Sel. (%)	Ref.
MoC _x @OMSF-10	340	4	85.9	98.3	S7
NiAl _{7/4}	340	4	54.6	99.9	S8
MoP/HY	300	4	85	99	S9
MoP/AC	300	4	82	99	S10
Ni-MFI-NSs	340	4	84.9	100	S11
MoP	300	4	>90	>90	S12
Mo ₂ C/AC	340	4	98	90	S13
Mo ₂ C/HY	300	3	95	81.4	S14
PMS-16	120	1.5	>99	>99	This work

Table S8. Selective hydrogenation of naphthalene catalyzed by different control catalysts on electrodes under closed-circuit operation^a

Entry	Anode	Cathode	Yield (%) ^b
1	[Co]	[Co]	0.63%
2	[Co]	[Ni]	3.67%
3	[Co]	[NiCo]	5.08%
4	[Ni]	[Co]	0.80%
5	[Ni]	[Ni]	0.99%
6	[Ni]	[NiCo]	1.66%
7	[NiCo]	[Co]	2.43%
8	[NiCo]	[Ni]	5.44%
9	[NiCo]	[NiCo]	8.12%

^aReaction conditions: naphthalene (0.1 mmol), catalyst (25.0 mol% based on Ni and Co), heptane (0.5 mL) and isopropanol (4 mL), 8 h, 120 °C, 1.5 MPa H₂. ^bDetermined by GC-MS.

Table S9. Selective hydrogenation of naphthalene catalyzed by different control catalysts on electrodes under open-circuit operation^a

Entry	Anode	Cathode	Yield (%) ^b
1	[Co]	[Co]	0.60%
2	[Co]	[Ni]	0.96%
3	[Co]	[NiCo]	1.58%
4	[Ni]	[Co]	0.61%
5	[Ni]	[Ni]	0.95%
6	[Ni]	[NiCo]	1.56%
7	[NiCo]	[Co]	0.61%
8	[NiCo]	[Ni]	0.97%
9	[NiCo]	[NiCo]	1.59%

^aReaction conditions: naphthalene (0.1 mmol), catalyst (25.0 mol% based on Ni and Co), heptane (0.5 mL) and isopropanol (4 mL), 8 h, 120 °C, 1.5 MPa H₂. ^bDetermined by GC-MS.

References

- S1 Z. Jian, G. Ming and C. Song, *Fuel Process. Technol.*, 2008, **89**, 467-474.
- S2 T. Tang, C. Yin, L. Wang, Y. Ji and F. S. Xiao, *J. Catal.*, 2008, **257**, 125-133.
- S3 S. C. Qi, L. Zhang, X. Y. Wei, J. i. Hayashi, Z. M. Zong and L. L. Guo, *RSC Adv.*, 2014, **4**, 17105-17109.
- S4 M. Fang, N. Machalaba, Sánchez-Delgado and A. Roberto, *Dalton Trans.*, 2011, **40**, 10621-10632.
- S5 M. Fang, N. Machalaba, Sánchez-Delgado and A. Roberto, *J. Catal.*, 2014, **311**, 357-368.
- S6 A. V. Bykov, D. V. Alekseeva, G. N. Demidenko, A. L. Vasiliev and L. Kiwi-Minsker, *Catalysts*, 2020, **10**, 1362.
- S7 M. Pang, X. Chen, Q. Xu and C. Liang, *Appl. Catal. A-Gen.*, 2015, **490**, 146-152.
- S8 X. Chen, Y. Ma, L. Wang, Z. Yang, S. Jin, L. Zhang and C. Liang, *ChemCatChem*, 2015, **7**, 978-983.
- S9 M. Usman, D. Li, R. Razzaq, M. Yaseen, C. Li and S. Zhang, *J. Ind. and Eng. Chem.*, 2015, **23**, 21-26.
- S10 U. Muhammad, D. Li, R. Rauf, L. Ullah, M. Oki, Y. Z. Hassan, B. A. Al-Maythalony, C. Li and S. Zhang, *J. Environ. Chem. Eng.*, 2018, **6**, 4525-4530.
- S11 P. Gong, B. Li, X. Kong, J. Liu and S. Zuo, *Appl. Surf. Sci.*, 2017, **423**, 433-442.
- S12 M. Usman, L. Dan, C. Li and S. Zhang, *Sci. China Chem.*, 2015, **58**, 738-746.
- S13 M. Pang, C. Liu, W. Xia, M. Muhler and C. Liang, *Green Chem.*, 2012, **14**, 1272-1276.
- S14 S. J. Ardakan and K. J. Smith, *Appl. Catal. A-Gen.*, 2011, **403**, 36-47.